vol. 57, pp. 791–802, 1975.
[10] S. L. Chuang and J. A. Kong, "Wave scattering from periodic rough surfaces," *Proc. IEEE*, vol. 69, pp. 1132–1144, 1981.
[11] A. Boström, "Surface waves on the periodic boundary of an elastic half space," *Appl. Sci. Res.*, vol. 39, pp. 129–142, 1982.
[12] F. L. Ng and R. H. T. Bates, "Null field method for waveguides of arbitrary cross section," *IEEE Trans. Microwave Theory Tech.*, vol. MTT-20, pp. 658–662, 1972.
[13] A. Boström and P. Olsson, "Transmission and reflection of electromagnetic waves by an obstacle inside a waveguide," *J. Appl. Phys.*, vol. 52, pp. 1187–1196, 1981.
[14] R. F. Millar, "The Rayleigh hypothesis and a related least-squares solution to scattering problems for periodic surfaces and other scatterers," *Radio Sci.*, vol. 8, pp. 785–796, 1973.

Anders Boström was born in Stockholm, Sweden, on November 2, 1951. He received the M.Sc. degree in engineering physics from Chalmers University of Technology, Göteborg, Sweden, in 1975, and the Ph.D. degree in mathematical physics from Chalmers University of Technology, Göteborg, Sweden, in 1980.

From 1980 until the present, he has been a Research Associate at the Institute of Theoretical Physics, Chalmers University of Technology. His main research interests are wave propagation and scattering of both electromagnetic and elastic waves, including such topics as multiple scattering, periodic structures, waveguides, and pulse scattering.

Microwave Automatic Impedance Measuring Schemes Using Three Fixed Probes

CHIA-LUN J. HU

Abstract—**Following a previous article reporting a general theory and a new approach using multiple probes to measure the complex impedance of an unknown microwave load, this article describes a simplified, but improved, design derived from that general theory. A simple analog dc signal processor was built according to this design and preliminary experiments were carried out to check the performance of the system. Real time oscilloscope displays showing the complex reflection coefficients of some standard loads and some time-varying loads were recorded. The performance of this system was checked against that of the standard traveling probe technique. The maximum disagreement between the two methods is about 5 percent in amplitude and 7° in phase. A special dc signal processor—the display rotator—was used in the system. The purpose, the design, and the performance of this rotator circuit are discussed in detail. Although the present experiments are restricted to fixed-frequency-automatic measurements, the system is seen to be easily generalized to step-frequency measurements as well. The latter can be used to record automatically the complex impedance spectrum of an unknown microwave load when the frequency is changed. Component imperfections that may affect the system accuracy and comparison of the present system with other automatic measuring systems are discussed.**

I. Introduction

MULTIPLE-FIXED probes mounted on a waveguide or a transmission line have been used by many investigators to measure the complex impedance $\overline{Z}$ of an unknown microwave load. A previous article published in this TRANSACTIONS [1] has summarized some of the background work in the field. Also in the article quoted, a novel approach that clarifies certain design confusions and that allows new designs to be reached was reported in detail. Following this new approach, static measurements (measurements of the outputs of the three probes with hand calculation to predict the unknown $\overline{Z}$ at different frequencies) and discussions of possible effects of system performance due to component imperfections were reported in several papers [2]–[4]. These static measurements verify, to a certain degree of accuracy, the theory reported in the quoted article. The theory is also verified by other investigators using digital means [5].

In the present article, the reader will see a simplified, but improved, design. Based on this new design, a dc electronic signal processor was built and tested. The detail of the design, the calibration, and the experimental result of this new approach will be discussed in order, following a brief review of the fundamental theory.

II. Theory

As reported in the quoted article [1], three fixed probes mounted on a lossless waveguide or a transmission line terminated by an unknown impedance $\overline{Z}_L$ (Fig. 1) can be used to measure automatically the phase and the magnitude of the complex $\overline{Z}_L$ at any fixed microwave frequency. The conditions that this measurement is made possible are

Manuscript received February 23, 1982; revised April 5, 1983. This work was supported by a grant from the National Science Foundation.

The author is with the Department of Electrical Sciences and Systems Engineering, Southern Illinois University, Carbondale, IL 62901.

0018-9480/83/0900-0756$01.00 ©1983 IEEE

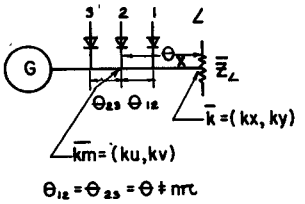

Fig. 1. Three probe automatic impedance measuring schemes.

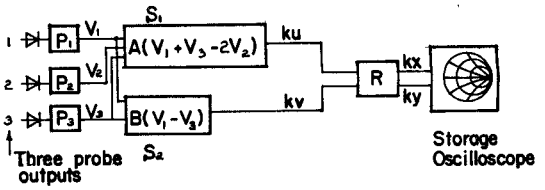

Fig. 2. Block diagram of dc signal processors.

the following:

1) The three probes are equally spaced, i.e., the round-trip phase distances θ_{12}, θ_{23}, in Fig. 1 are equal and $\theta_{12}=\theta_{23}\neq n\pi$.

2) The three detecting diodes are operated in square-law regions.

3) All probes do not load the waveguide and do not have mutual coupling.

The validation of these conditions in practical systems is to be discussed in a later section. Under these conditions, the author has shown that the real and the imaginary parts (k_u, k_v) of the unknown reflection coefficient $\bar{k}_m$ under the central probe can be expressed by the following equations (the derivation of these equations from a slightly different point of view is given in Appendix I):

$$k_u=\left(e_1^2+e_3^2-2e_2^2\right)/4(\cos\theta-1) \tag{1}$$

$$k_v=\left(e_1^2-e_3^2\right)/4\sin\theta \tag{2}$$

where e_i^2 are the probe outputs normalized with respect to the forward power in the waveguide. θ is the round-trip phase distance between the adjacent probes, as shown in Fig. 1. From these equations, we can calculate immediately the real and imaginary parts k_x, k_y of the unknown reflection coefficient $\bar{k}$ at the loading point (Fig. 1) by the following matrix equation:

$$\begin{bmatrix}k_x\\k_y\end{bmatrix}=\begin{bmatrix}\cos\theta x & \sin\theta x\\ -\sin\theta x & \cos\theta x\end{bmatrix}\begin{bmatrix}k_u\\k_v\end{bmatrix} \tag{3}$$

where θx is the round-trip phase distance between the central probe and the loading point. The $2\times 2\ \theta x$-matrix here is just a rotation matrix which represents the rotation of the phasor $\bar{k}_m$ in the complex plane by an angle equal to θx.[1]

It is to be noted here that, at any fixed frequency, both θ and θx in (1), (2), and (3) are constants. Therefore, to implement these equations with electronic circuits is quite simple. It involves only weighted adders and subtractors as described in the following section.

III. Design

This section will be devoted to the general design approach and the design of a special "rotator" circuit for implementing (1), (2), and (3) above.

Fig. 2[2] is the block diagram of the dc signal processor designed. P_1, P_2, and P_3 represent three precision low-drift preamplifiers used to boost the dc probe output voltages from millivolt range to tenth-of-a-volt range. Adjusting the gains of P_1, P_2, and P_3, one can make the overall sampling ratios of the three probes the same without adjusting the probes mechanically. S_1 and S_2 in Fig. 2 represent two weighted (op-amp) adders designed to implement (1) and (2). By adjusting the gain controls A, B of these two adders, one can calibrate the coefficients or the denominators of the right-hand sides of (1) and (2).

It is to be noted here that if the power output of the microwave generator is very stable, then the normalization process mentioned under (1) and (2) can be absorbed by the adjustment of coefficients A, B here. Actually, the normalization is needed only when the power level of the generator is fluctuating in time or when we intend to scan the power level to measure the *nonlinear* properties of the microwave load.

The "rotator" R in Fig. 2 represents the signal processor used to implement (3). As mentioned earlier, at any fixed frequency, θ_x is a constant. Hence, (3) can actually be implemented by just another pair of weighted adders with weighting factors properly calibrated. However, in practice, this calibration is very cumbersome, if not too difficult, because 1) there are definite relationships among the four coefficients in the θ_x-matrix, and 2) each coefficient must be related in a definite way to the phase distance θ_x shown in Fig. 1.[3] Consequently, we must seek a better design to avoid these calibration difficulties.

If we divide the θ_x-matrix in (3) by $\cos\theta_x$, the equation becomes

$$\begin{bmatrix}k_x\\k_y\end{bmatrix}=\cos\theta_x\begin{bmatrix}1 & K\\ -K & 1\end{bmatrix}\begin{bmatrix}k_u\\k_v\end{bmatrix} \tag{4}$$

where $K\equiv\tan\theta_x$. This means that we have two weighted adders with one common gain control factor $\cos\theta_x$ and one

[1]The rotation matrix can actually be eliminated by rotating the Smith Chart overlay *reversely* if we connect k_u, k_v outputs *directly* to the x, y inputs of the display oscilloscope. This was first discussed in the paper by Hu [1] which is suitable solely for a single-frequency measurements. However, for step-frequency measurements which will be described in Section VI, this rotation matrix must be implemented electronically because the Smith Chart must remain fixed on the scope when the frequency is stepped automatically.

[2]Standard buffer circuits (not shown in Fig. 2) are used in the system built. These circuits are used to avoid loading effects between stages.

[3]With a good microcomputer, (3) is probably much easier to implement if the cost is not of primary concern. The author is currently working on this point. There are also some four-quadrant $\cos\theta$, $\sin\theta$ analog devices available in the market which may be used in implementing the θ_x-matrix here. But they are, generally, quite cumbersome to adjust if high accuracies are demanded.

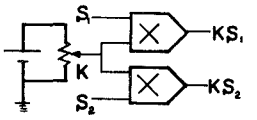

Fig. 3. Display rotator using multiplier circuits.

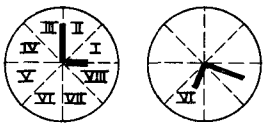

Fig. 4. Sample displays before and after rotation.

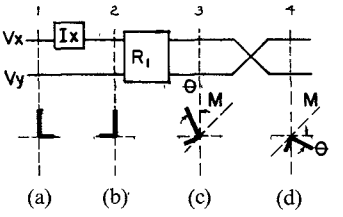

Fig. 5. A possible patching of the rotator to achieve the rotation described in Fig. 4.

common weighting factor K that must be synchronously adjustable. The common gain control factor just changes the scale of the $\bar{k}$-phasor displayed on the oscilloscope. It is much easier to calibrate as will be seen later. But the common weighting factor K determines very sensitively the accuracy of the phase angle of $\bar{k}$ and it is not that easy to adjust because of the synchronism requirement. Nevertheless, this synchronous adjustment can be achieved by using two multiplier circuits as shown in Fig. 3 or by using a dual-potentiometer in a dual-adder (that is, we can design two op-amp adders with gains synchronously controlled by the adjustment of a dual-pot). The latter is much cheaper but, generally, not very accurate as far as synchronism is concerned. However, with some trimmer adjustment and a special calibration technique to be reported later, it is found that this dual-pot approach is quite adequate for medium accuracy measurements.

There is another important practical problem in implementing (4). Because the value of θ_x (Fig. 1) may fall into any of the four quadrants if the microwave frequency is arbitrary, K in (4) may be any positive or negative number including $\pm\infty$. To implement this K factor by simple weighted adders is very difficult not only because the weighted factor of a common op-amp adder cannot be adjusted from 0 to $\pm\infty$, but also because the sign of K depends on the value of θ_x of the microwave frequency chosen. Nevertheless, by using a special "patching" technique comparable to that used in an analog computer, as discussed below, this problem is practically solvable.

Suppose we build two inverter circuits I_x and I_y with $V_{out} = -V_{in}$ for any analog input V_{in}'s, and also suppose we build a 45° rotator R that can rotate the display on the oscilloscope by an angle θ adjustable between 0° and 45°.[4] Then with proper patching of these three circuits we can rotate the display on the scope by any angle beyond 45°. Below is one example.

Suppose the display on the scope without the rotator is a boldface $\boldsymbol{L}$ as shown in Fig. 4(a) and we want to rotate this display electronically to the position shown in Fig. 4(b). The following is a possible-patching for achieving this.

Let the original signals fed to the x, y inputs of the scope be called V_x and V_y. Then we can first connect V_x to an inverter I_x, as shown in Fig. 5. The display monitored at port 2 of Fig. 5 will be an x-inverted "$\boldsymbol{L}$", as shown in Fig. 5(b). Secondly, we can connect the 45° rotator R to port 2 and the display monitored at port 3 will be that as shown in Fig. 5(c) where $\theta < 45°$ and $> 0°$. Now if we switch the two outputs at port 3, as shown in Fig. 5, then the display monitored at port 4 will just be the mirror image of Fig. 5(c) across the diagonal line M as shown in Fig. 5(d). This last display is the same as that shown in Fig. 4, or the rotated image we want.

If we denote the cascaded connection or the patching in Fig. 5 by $I_x RS$, where S means switching of x, y terminals, then we can easily verify that proper patchings for all possible rotations of displays should be those shown in Table I. In this table, the first column is the sector that the required angle of rotation falls into. The sector numbers are those shown in Fig. 4. The equal signs in the table relate all possible patchings that may be used to reach the same rotation. The example given above is shown by the sixth line in the table.

IV. Calibration

The general calibration steps of the system are the following.

1) Adjust the offsets of all op-amps in the circuit shown in Fig. 2 such that when the input of each op-amp is grounded, its output is zero.
2) Connect a movable short to the waveguide loading point. Adjust the gain of each pre-amp P_1, P_2, or P_3 such that when the short is moved in and out, the output of each pre-amp varies from zero volt to the same maximum level for all three pre-amps. This ensures that the overall sampling ratios of the three probes are the same even though physically the penetration depths of the probes may be different.
3) Adjust the weighting factors in the adders S_1 and S_2 (Fig. 2) by grounding all inputs except one and monitoring the outputs.
4) Connect the inputs of S_1 and S_2 to the outputs of P_1, P_2, and P_3. Then connect the outputs of S_1 and S_2 to the x, y input of the storage scope. With the movable short moving in and out, the scope should display a good round circle with the center of the circle coinciding with the center of the scope. Gain adjustments for S_1 and S_2 may be necessary to bring the circle to a standard size fitting to, for example, the circumference of a Smith Chart overlay.

[4] This can be achieved by implementing (4) with $0 \leq K \leq 1$ which can be done with a single dual-pot complemented by some fine-tuning trimmers as just described.

TABLE I
POSSIBLE PATCHINGS FOR ALL POSSIBLE ROTATIONS

I.	R
II.	$SRI_x = I_yRS$
III.	$RSI_x = SI_xR = RI_yS = I_ySR$
IV.	$I_xRI_y = I_yRI_x$
V.	$I_xI_yR = I_yI_xR = RI_xI_y = RI_yI_x$
VI.	$I_xRS = SRI_y$
VII.	$RI_xS = I_xSR = RSI_y = SI_yR$
VIII.	$SRS = I_xRI_x = I_yRI_y$

Explanation: Roman numbers: Angle of rotation desired. (see Fig. 4)

R: Rotator that can make 0° to 45° rotation

S: Switching of x,y outputs

I_x, I_y: Inverters for x,y outputs

5) The location of the beam spot when the movable short is pushed all the way in to the loading point determines the angle we need to rotate by the rotators. That is, we need to bring this spot to the leftmost point on the Smith Chart. Depending on the angle we need to rotate, we should select a proper patching from Table I and connect the output of the rotator to the scope. With coarse tuning (by adjusting the dual-pot) and fine tuning (by adjusting the trimmer) we can not only bring the beam spot to the leftmost point when the short is at the loading point, but also trim the "circle" to a perfect round shape when the short is moved in and out.
6) The size of the circle after the rotation generally does not fit any more to the Smith Chart circumference. Gain adjustments at the outputs of the rotator are necessary to bring the circle back to the standard size.

When every step described above is carried out properly, the display traced on the scope should have the following properties.

a) When the short is at the loading point, the beam spot is at the leftmost point on the circle.
b) When the short is moved in and out, the beam spot should trace a good circle centered at the center of the scope.
c) When the short is pulled out, the beam spot should go counterclockwise. This is so because when the short is moved away from the loading point, the loading point is relatively moving towards the generator. Consequently, according to the Smith Chart, the measuring point should move towards the generator or move counterclockwise.
d) When nothing is changed, but the movable short is replaced by a matched load (or a terminator), the beam spot should locate right at the center.

When all the above displays are met, the circuit is properly calibrated for measurements of any unknown loads at the fixed frequency used.

V. EXPERIMENTS

The microwave generator used in the author's experiment is an HP 8620C/86250D sweep generator (maximum power 10 mW) operated at CW fixed-frequency mode. The display oscilloscope is a Tektronic 5403/D41 storage oscilloscope. The probes used are HP 444A wide-band nonresonating probes. The waveguide is in *X*-band and the separation between the adjacent probes is 40 cm (± 0.5 mm). The central probe is about 100 cm away from the loading point. The probe penetration depths are adjusted such that the probe outputs are not to exceed 10-mV dc when the movable short is moved in and out. An attenuator and an isolator are connected between the generator and the main waveguide. The microwave frequency is measured by a frequency meter. The frequencies used in the author's experiments are 9, 10, and 11 GHz. For the electronic dc signal processor, the pre-amps used are OP-07E. These pre-amps are designed to amplify the signals by 100 to 250 times with adjustable gains. After proper calibration, typical results at 10 GHz are shown in Figs. 6–9. Results at other frequencies are quite similar to these. Fig. 6 is the stored trace of the beam spot on the storage scope when a movable short is gradually pulled out from the loading point. The beam spot starts at the leftmost point on the circle. It traces a counterclockwise circle when the short is pulled out. The circle was traced repeatedly two to three times before the short comes to an end, depending on the frequency used.

Fig. 7 shows the result that when nothing is changed except that the movable short is replaced by a matched load, the beam spot falls right at the center of the circle which is the trace for the movable short. Fig. 8 shows that when this matched load is detached from the waveguide and moved away from the waveguide, the beam spot starts at the center and spirals into a point corresponding to the open-end impedance of the waveguide. Fig. 9 shows the result of the author's palm (used as load) concealing the open end of the waveguide and then moving away from

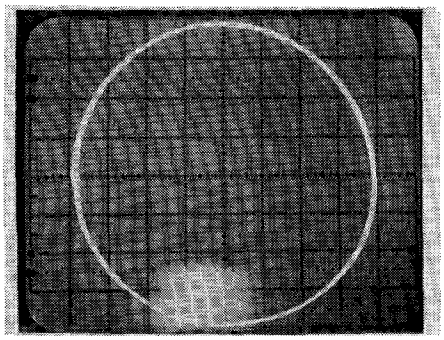

Fig. 6. Display due to a moving short.

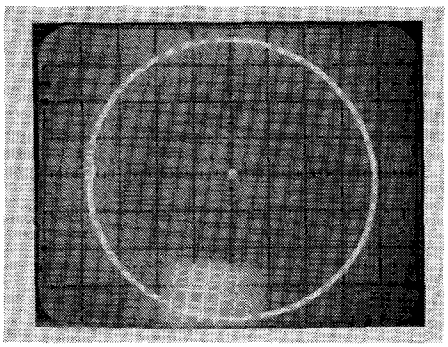

Fig. 7. Superimposed displays due to a moving short and a matched load.

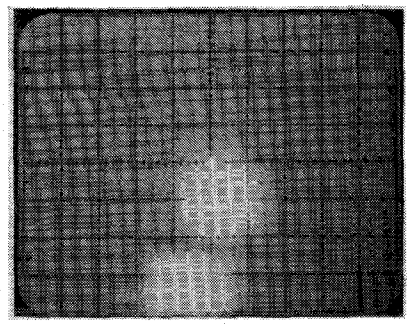

Fig. 8. Display when the matched load is moved away from the loading point.

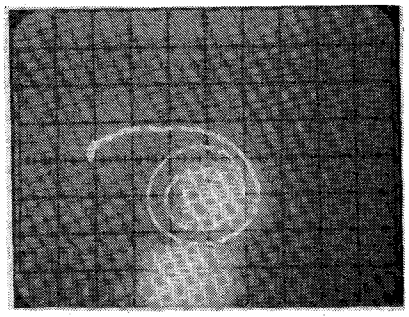

Fig. 9. Display when the author's palm is moved away from the loading point.

the waveguide. The beam spot starts at the left end of the display and spirals again into the point corresponding to the open-end impedance. These pictures were repeatable at a fixed frequency as far as the circle, the central spot, and the point corresponding to the open-end impedance are concerned.

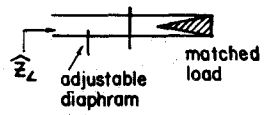

Fig. 10. Simmulated load.

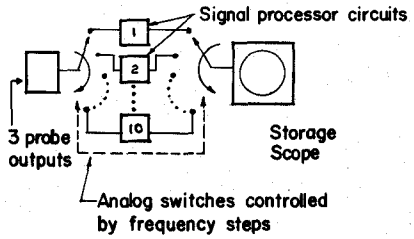

Fig. 11. Step frequency impedance measuring scheme.

The second group of experiments was done to check the accuracy of measurements numerically. A simulated load is used. This load consists of an adjustable diaphragm terminated by a matched load as shown in Fig. 10. At different diaphragm depth and different frequencies, the unknown reflection coefficient $\bar{k}$ was first measured by the automatic-display system described above. Then it was measured by the standard traveling probe technique. The maximum discrepancy recorded between the two results is that the magnitude "error" is about 5 percent and the phase "error" is 7°. It is the author's belief that when a digital means or a desktop computer is used to implement the system, the "accuracy" or agreement should be much more improved because a signal-averaging process can be programmed such that possible random fluctuations in the measurements are averaged out.

VI. Step-Frequency Scheme

The measuring scheme discussed above is a fixed-frequency automatic impedance measuring scheme. A very prominent point of this scheme is that there is no restriction imposed on the separations between the adjacent probes as long as they are equal and not equal to $n\pi$. Therefore, as long as we set the physical distances between the adjacent probes equal and select the microwave frequency to avoid $\theta = n\pi$ condition, the same circuit described above can be used at any frequencies if a proper calibration is carried out at each different frequency. That is, we can select, say, ten frequencies in, say, the X-band, for which $\theta \neq n\pi$, and build ten identical circuits such that each is calibrated at each frequency selected. Then we can program the sweep generator to generate a microwave signal with frequency stepped as we selected and design an analog switching circuit as shown in Fig. 11, such that whenever the frequency is stepped, there is always a properly calibrated circuit switched in place to process the signals from input to output. Consequently, the display on the scope will be a dotted curve which will be the complex impedance spectrum of $\bar{Z}$ under a Smith Chart when the frequency is stepped.

VII. Discussion

A. Probe-Coupling and Probe Loading-Effect

As mentioned in the last section, the main design equations (1), (2) are not restricted to any probe separation except when $\theta = n\pi$. Therefore, we can put the probes very far apart to minimize the probe-coupling effect. In the author's experiments reported above, the probes are set at approximately 40 cm apart which is equal to 9 to 12 guided wavelengths at the frequencies used. Probe-coupling, probe-resonance, and probe-loading effects are negligible as tested by monitoring one probe output while pulling other probes out from the waveguide. The monitored output does not change after the probes are pulled out. The physical penetrations of all probes in the waveguide are examined and they are all less than 1 mm. The loading effect, even if it exists, can be eliminated by increasing the power output from the generator and withdrawing the probes further from the main guide. But the author found that with 10–20-mW power sent out from the generator, no appreciable loading effect is observed.

B. Nonsquare-Law Diode Response

If the power is not swept, we can always gradually pull the probe out from the waveguide until that the maximum dc probe output is less than 15 mV when a movable short is moved in and out. For most microwave detection diodes, square-law is well followed under this output voltage range. On the other hand, if we intend to sweep the power of the generator for nonlinear measurements we should not only design a normalization circuit as mentioned under (2) in Section II, but we should also design three square-law correction circuits to correct the deviations of the diode responses from perfect square-law at higher power levels. Many "function-generating" circuits used in analog computers which yield "any" desired dc input–output relations can be used here to correct the deviation. These circuits are diode circuits and their input–output responses can be programmed to fit to "any" desired curves.

C. Relation to the 6-Port Schemes

As shown in Appendix I, the design equations (1), (2), and (3) stated in Section I can be derived from the "power equations" (A1), (A2), and (A3) stated in the Appendix. These power equations are actually a special case of the 6-port equations [6] if we normalize the 6-port equations with respect to the forward power. Equations (A1), (A2), and (A3) are written under the assumption that probe-loading and probe-coupling effects are not taken into account. This is acceptable in most practical applications where only medium accuracies in measurements are required. However, if higher accuracies are demanded, the probe-loading and probe-coupling effects cannot be neglected and the coefficients in (A1), (A2), and (A3) cannot be considered as just one or $e^{\pm j\theta}$. These coefficients may be, say, $1.005e^{-j0.01}$ and $0.99e^{\pm j(\theta-0.01)}$, etc. Consequently, we must use the general 6-port approach to design the signal-processing scheme. One very significant point of the general 6-port scheme is that it takes all loading and coupling effects into account as long as the dependencies among the ports are linear. So theoretically these effects, no matter how strong they are, will not affect the accuracy of the measurements in a well-calibrated 6-port scheme.

VIII. Conclusion

We see that the automatic impedance measuring schemes reported here are derived from a completely different point of view from those used in the hetrodyne schemes. It is much closer to the 6-port schemes reported in the literature, although originally these two were derived from quite different approaches. The advantages of the scheme reported in this article may be summarized in the following.

1) The signal processing is at dc level. Therefore, it is much easier to build and the cost is much lower.

2) It is a real-time measuring scheme. That is, it can track and record any change of the complex impedance when the load is changed in time.

3) It can be used in either fixed-frequency measurements or step-frequency measurements. A complex impedance spectrum can be recorded if step-frequency scheme is used.

4) It may be used in nonlinear measurements if proper normalization and square-law correction are used.

5) The circuit is very simple and very inexpensive. The calibration is also quite simple to carry out at a fixed frequency.

Appendix I
Derivation of the Design Equations (1), (2) in Section II

If the reflection coefficient under the central probe is denoted by $\bar{k}_m$ and $\bar{k}_m = ke^{j\Phi}$, then the square of the normalized total field sampled by the central probe is

$$e_2^2 = |1 + \bar{k}_m|^2 = 1 + k^2 + 2k\cos\Phi. \quad \text{(A1)}$$

The square of the normalized total field sampled by probe 1 is

$$e_1^2 = |1 + \bar{k}_m e^{-j\theta}|^2 = 1 + k^2 + 2k\cos(\Phi - \theta). \quad \text{(A2)}$$

Similarly

$$e_3^2 = |1 + \bar{k}_m e^{+j\theta}|^2 = 1 + k^2 + 2k\cos(\Phi + \theta). \quad \text{(A3)}$$

Applying the operations (A2)+(A3)−2(A1) and (A2)−(A3) to these three equations, one can arrive at (1), (2) in Section II immediately.

References

[1] C. J. Hu, "A novel approach to the design of multiple-probe high-power microwave automatic impedance measuring schemes," *IEEE Trans. Microwave Theory Tech.*, vol. MTT-28, no. 12, pp. 1422–1428, Dec. 1980.

[2] ——, "An improved design of the swept-frequency, automatic impedance measuring schemes using multiple-probes," in *Proc. 1981 Int. Microwave Symp.*, Los Angeles, CA, May 28, 1981.

[3] ——, "Design of signal processors for automatic impedance measuring schemes using fixed probes," in *Proc. 19th Automatic RF Techniques Group Meeting*, Dallas, TX, June 19, 1982.

[4] ——, "Experiments on *X*-band automatic impedance measuring schemes using three fixed probes," in *Proc. 20th Automatic RF Techniques Group Meeting*, Boulder CO, Nov. 5, 1982.

[5] E. Martin, J. Margineda, and J. Zamarro, "An automatic network analyzer using a slotted line reflectometer," *IEEE Trans. Microwave Theory Tech.*, vol. MTT-30, no. 5, pp. 667–669, May 1982.
[6] G. F. Engen, "Determination of microwave phase and amplitude from power measurements," *IEEE Trans. Instrum. Meas.*, vol. IM-25, pp. 414–418, Dec. 1976.

Chia-Lun J. Hu received the B.S.E.E. degree from the National Taiwan University, Taipei, in 1958, the M.S.E.E. degree from the National Chiao-Tung University, Hsinchu, Taiwan, in 1960, and the Ph.D. degree from the University of Colorado, Boulder, in 1966.

From 1960 to 1963 he was an Engineer at the Broadcasting Corporation of China and, subsequently, an Instructor at the Chiao-Tung Graduate School. In 1963 he received a NASA–Chinese Government Scholarship to pursue his doctoral studies at the University of Colorado, Boulder. Since 1966 he has assumed various research and teaching positions at the University of Colorado, the Jet Propulsion Laboratory, and the Chiao-Tung University. He is currently a Professor in the Electrical Sciences and Systems Engineering Department, Southern Illinois University. His research interests include electrooptics, bioengineering, air pollutant detection, and automatic microwave measurements. He published 35 papers in these and other fields. He has been either a principal or a coprincipal investigator under five government grants supporting his research in these fields.

A General-Purpose Program for Nonlinear Microwave Circuit Design

VITTORIO RIZZOLI, MEMBER, IEEE, ALESSANDRO LIPPARINI, AND ERNESTO MARAZZI

Abstract—**The paper describes the basic philosophy and the general structure of a user-oriented program package capable of designing broad classes of nonlinear microwave subsystems. Some of the peculiar aspects of the nonlinear design problem and the computer solutions adopted are discussed in detail. The application to a practical medium-power oscillator shows that the program is numerically efficient and yields well-defined and accurate results. Furthermore it provides full coverage of several aspects of circuit performance that were previously treated by empirical approaches, such as detailed effects of higher harmonics, active device operating temperatures, and circuit regulations.**

I. INTRODUCTION

THE COMPUTER-AIDED design (CAD) of linear microwave circuits can be considered a well-settled matter, as is shown by the extensive technical literature on this subject, and by the commercial availability of powerful general-purpose CAD programs [1]. On the other hand, the general problem of nonlinear circuit design still represents a challenge for the microwave engineer, owing to its much higher difficulty: in fact, in this case, carrying out a design means finding a network and a nonsinusoidal electrical regime which satisfies the design specifications, that this network must be able to support.

The primary purpose of this paper is to describe the structure and basic philosophy, and to illustrate an example of the practical application of a program package allowing straightforward MIC designs to be carried out within a class of active nonlinear subsystems having the general topology shown in Fig. 1. In the current version of this program the nonlinearity is confined to the presence of a user-defined nonlinear "component" having a maximum of 3 ports and usually consisting of a set of semiconductor chips: possible combinations are, for example, one transistor (either bipolar or FET), one or two diodes, or one transistor and one diode. The remaining blocks are representative of linear subnetworks and are labeled according to their physical meaning:

- *L* linear elements (if any) of chip equivalent circuits;
- *S* set of movable short-circuit connections allowing any chip mount configuration to be selected (e.g., common source or gate for an FET chip);
- *P* package or mounting parasitics;
- *M* MIC (usually microstrip) network including load, dc bias, and possibly a number of independent sinusoidal sources harmonically related to the fundamental frequency of operation (e.g., the pump in a frequency divider).

Manuscript received February 28, 1983; revised May 3, 1983. This work was partly sponsored by the Italian National Research Council [CNR].

V. Rizzoli and A. Lipparini are with the Dipartimento di Elettronica, Informatica e Sistemistica, University of Bologna, Villa Griffone, Pontecchio Marconi, Bologna, Italy.

E. Marazzi is with the SIAE Microelettronica, S.p.A., Via Buonarroti 21, Cologno Monzese, Milano, Italy.

0018-9480/83/0900-0762$01.00 ©1983 IEEE